

## Optical dephasing and migration of bound excitons in GaP:N

W. S. Brocklesby

*Clarendon Laboratory, University of Oxford, Parks Road, Oxford, OX1 3PU, United Kingdom*

R. T. Harley

*Clarendon Laboratory, University of Oxford, Parks Road, Oxford, OX1 3PU, United Kingdom  
and GEC Research Limited, Hirst Research Centre, Wembley, Middlesex HA9 7PP, United Kingdom*

A. S. Plaut

*Clarendon Laboratory, University of Oxford, Parks Road, Oxford, OX1 3PU, United Kingdom*

(Received 28 January 1987)

Saturation spectral hole-burning techniques have been used to investigate optical dephasing of the  $B$  state ( $J=2$ ) of bound excitons in GaP:N between 1.5 and 4.2 K. Above 2 K dephasing is thermally activated with activation energy 0.88 meV corresponding to the splitting to the  $A$  state ( $J=1$ ). Below 2 K the dominant dephasing mechanism appears to be temperature independent and, on the basis of its energy and concentration dependence, is assigned to exciton hopping between different nitrogen centers. We compare these results with earlier measurements on  $NN_i$  centers in GaP and with photon-echo dephasing measurements on the  $A$  state by Molenkamp and Wiersma.

### I. INTRODUCTION

Optical dephasing of localized and bound exciton states in semiconductors is important because of its relevance to the nonlinear optical response and because of the insight it gives into exciton dynamics. In general, at high temperatures excitonic resonances are thermally broadened as a result, for example, of phonon-induced excitation to the free-carrier continuum.<sup>1</sup> At low temperatures, even when recombination is dipole allowed, dephasing is frequently not determined by the recombination time but is limited by some faster process. For example, localized heavy-hole excitons in GaAs quantum wells have dephasing times of order 30 ps compared to radiative lifetimes of order 500 ps,<sup>2,3</sup> and bound excitons in the  $A$  state of GaP:N have dephasing times of  $\sim 25$  ps determined by phonon emission compared to radiative lifetimes of 38 ns.<sup>4</sup> This rapid dephasing for excitons is in contrast to observations in color-center systems where lifetime broadening is frequently dominant at low temperatures.<sup>5</sup> We report here an investigation of optical-dephasing mechanisms for the dipole-forbidden  $B$  state of GaP:N which permits study of phenomena occurring on time scales much longer than the previous  $A$ -state measurements.<sup>4</sup>

The spectroscopy of the isoelectronic impurity system GaP:N has been extensively studied following pioneering work by Thomas and Hopfield<sup>6</sup> and Cuthbert and Thomas.<sup>7</sup> At low temperatures there are groups of zero-phonon absorption and luminescence lines between 567 and 535 nm which are associated with excitons bound to isolated nitrogen atoms ( $N$  lines) and to various other centers believed to involve nitrogen pairs at varying separations ( $NN_i$  lines, where  $i$  ranges from 1 to  $\sim 10$ ). In weakly doped material ( $[N] \sim 10^{15} - 10^{17} \text{ cm}^{-3}$ ) the emis-

sion spectrum is dominated by two  $N$  lines,  $A$  and  $B$  [see Fig. 1(a)] near 535 nm, associated, respectively, with  $J=1$  and  $J=2$  exciton states. The  $A$  line ( $\lambda=534.85$  nm) is electric-dipole allowed and has a radiative lifetime of 38 ns, whereas the  $B$  line, which lies  $\sim 0.88$  meV lower in energy ( $\lambda=535.06$  nm), is forbidden and has a radiative lifetime of  $4 \mu\text{s}$ .<sup>7</sup> The  $A$  line has a binding energy of 10 meV with respect to a free exciton. The  $V$  band [see Fig. 1(a)] has been shown by Gershoni *et al.*<sup>8</sup> to be an inhomogeneously broadened envelope of zero-phonon transitions of excitons bound to single nitrogen centers, weakly perturbed by distant impurities. Absorption spectra usually show only the allowed  $A$  line, although the  $B$  line can be observed by luminescence excitation (see Sec. II). In heavily doped material ( $[N] \sim 10^{18} \text{ cm}^{-3}$ ) the  $A$  and  $B$  lines are relatively weak or are missing from the emission spectrum which is dominated by the  $NN_i$  features [see Fig. 1(b)]. This is a result of efficient nonradiative energy transfer and relaxation between different binding centers.<sup>9</sup> In such heavily doped samples there may also be a Stokes shift between absorption and emission in the  $A$  line due to spatial and spectral migration of energy within the inhomogeneously broadened profile.<sup>10</sup> The strongest exciton binding, 143 meV with respect to a free exciton, occurs for the  $NN_1$  centers associated with [110]-oriented  $N$  pairs in nearest-neighbor  $P$  sites. The other  $NN_i$  centers ( $i > 1$ ) form a converging series towards the isolated nitrogen  $N$  lines. The  $NN_i$  features show division into  $A$ -like and  $B$ -like lines<sup>6</sup> with lifetimes comparable to their  $N$  counterparts,<sup>11</sup> but in these cases small crystal-field splittings within  $J=1$  and  $J=2$  states can be resolved.

In this paper we describe a study of saturation spectral hole burning in the  $B$  state of single nitrogen centers in low-concentration material ( $[N] \sim 10^{15} - 10^{17} \text{ cm}^{-3}$ ).

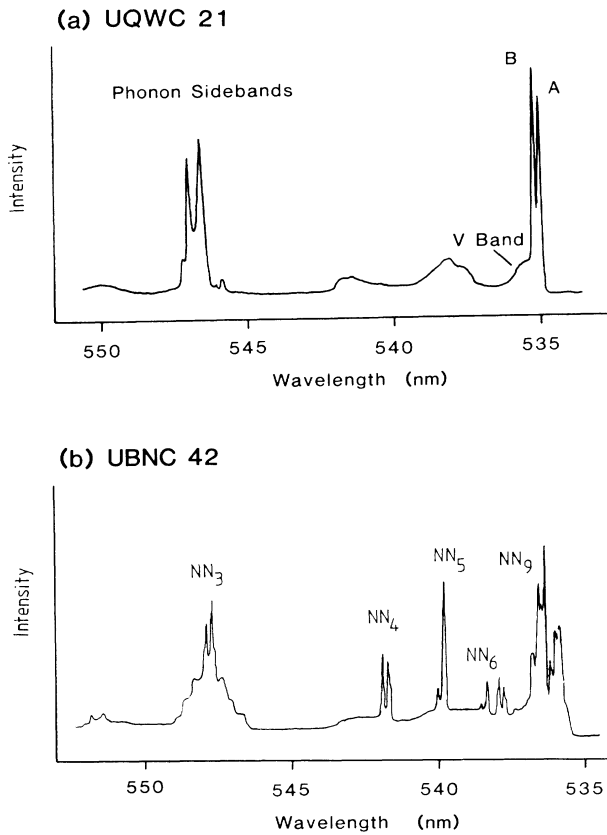


FIG. 1. Luminescence spectra at 4.2 K of GaP:N samples containing (a)  $4 \times 10^{16} \text{ N cm}^{-3}$  and (b)  $1.5 \times 10^{18} \text{ N cm}^{-3}$ .

The measurements enable us to determine the homogeneous linewidth and hence the dephasing time for the  $B$  state at temperatures between 1.5 and 4.2 K and as a function of position in the inhomogeneous line profile. At very low temperatures dephasing is dominated by phonon-assisted hopping of excitons on a time scale of order 800 ps between different binding centers even for nitrogen concentrations  $[N]$  as low as  $4 \times 10^{15} \text{ cm}^{-3}$  (mean spacing  $\sim 600 \text{ \AA}$ ). As the temperature is increased phonon-induced  $B$ -to- $A$  transitions on a single center become dominant. These conclusions are compared with a previous hole-burning study of the  $NN_1$  center in high-concentration material.<sup>12</sup> They also lead to some reinterpretation of recent optical-dephasing measurements of the  $A$  state using photon-echo techniques by Molenkamp and Wiersma.<sup>4</sup>

## II. EXPERIMENTAL METHODS AND MEASUREMENTS

Three samples have been used in the experiments, as detailed in Table I. Concentrations of nitrogen were determined from the  $A$ -line absorption following the work of Lightowers *et al.*<sup>13</sup> Results obtained from the epitaxial sample 2-527 were qualitatively similar to those from the bulk sample UQWC21 although less detailed due to reduced signal-to-noise ratio. We therefore concentrate on results from the two bulk samples, UQWC21 and L1, which differ in nitrogen content by a factor 10. The samples were mounted, as far as possible free from strain, in a helium cryostat either immersed in liquid helium pumped to temperatures below the  $\lambda$  point or surrounded by exchange gas. Temperatures were measured either using a Au-Fe-Cu thermocouple or a 220- $\Omega$  Allen-Bradley carbon resistance thermometer calibrated *in situ* against helium vapor pressure.

The complete apparatus for optical measurements is shown in Fig. 2. It consists of two independent, argon-ion-pumped, cw single-mode, Rhodamine-110 dye lasers with linewidth  $\sim 2 \text{ MHz}$  (CR 599-21), whose beams are superimposed using a 50/50 beam splitter and illuminate the sample in a collinear geometry. A few percent of each dye laser beam is split off to provide a monitor both of mode structure using confocal Fabry-Perot spectrum analyzers and of wavelength using a wave meter. The latter provides absolute readings to  $\pm 5 \times 10^{-3} \text{ nm}$ . The intensity of the combined laser beams is monitored just before the sample using a photodiode and beam splitter (not shown in the diagram). Luminescence from the sample is collected at  $90^\circ$  to the incident beam and is analyzed using a 0.5 m monochromator with a cooled photomultiplier. Signals from the photomultiplier are normalized to the incident beam intensity and displayed directly on an oscilloscope or recorded in a signal averager.

Figure 1 shows luminescence spectra excited using  $15 \text{ W/cm}^2$  of 514.5 nm light from one of the argon lasers. Figure 3 shows a more detailed measurement of the  $B$ -line luminescence for the two bulk samples. Also shown in Fig. 3 are luminescence excitation spectra obtained by tuning just one of the dye lasers through the  $B$ -line region while detecting emitted light at  $547.0 \pm 0.2 \text{ nm}$ , the wavelength of the phonon sidebands indicated in Fig. 1(a). These sidebands contain components associated with both  $A$  and  $B$  zero-phonon lines as can be seen from study of Fig. 4, which shows the variation in the sideband emission spectrum at 4.2 K for resonant excitation (a) on the high-energy side, (b) just below line center, and (c) in the low-energy tail of the  $B$  line. It can

TABLE I. GaP:N sample characteristics.

Sample No.	$[N] (\text{cm}^{-3})$	Form	Origin
UQWC21	$4 \pm 2 \cdot 10^{16}$	Bulk	Bell Labs.
2-527	$7 \pm 3 \cdot 10^{16}$	Epilayer on GaP	Bell Labs.
L1	$4 \pm 2 \cdot 10^{15}$	Bulk	Kings College

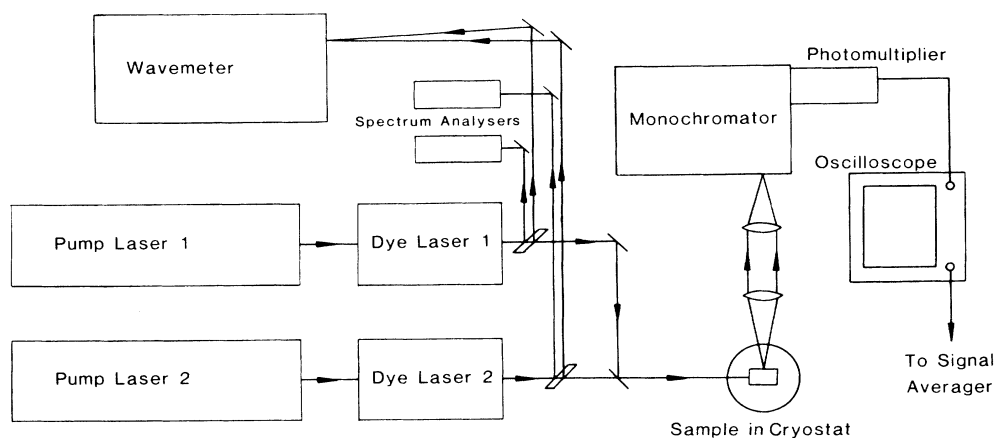


FIG. 2. Apparatus for photoluminescence, photoluminescence excitation, and saturation hole-burning measurements. For details see text.

be seen that detection at 547 nm gives some discrimination between *B* and *A* absorption.

The spectra of Fig. 3 show a shift of  $\sim 0.4$  meV to lower energy between absorption and emission. We have considered the rather trivial possibility that this may result from resonant reabsorption of *B*-line emission by *A*

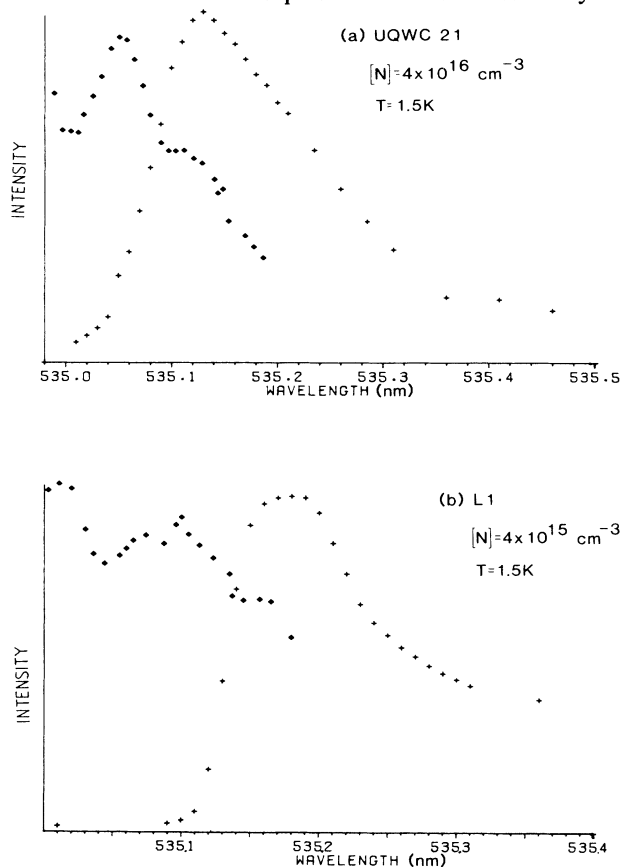


FIG. 3. Luminescence (crosses) and luminescence excitation (dots) spectra of samples containing (a)  $4 \times 10^{16} \text{ N cm}^{-3}$  and (b)  $4 \times 10^{15} \text{ N cm}^{-3}$ . Increase of luminescence excitation below  $\sim 535.0$  nm is due to the strong *A*-line absorption at 534.85 nm.

states at centers in the tail of the inhomogeneous profile, but the *A*-line absorption tail is about an order of magnitude too weak to account for the observed emission line shape. In addition, the rate of energy transfer by this process would be limited by the *B*-state radiative lifetime ( $\sim 4 \mu\text{s}$ ) whereas the spectral-hole-burning measurements, described below, indicate energy transfer occurring on a time scale of  $\sim 800$  ps.

Saturation spectral hole burning is measured using dye laser 2 (Fig. 2) as a pump at fixed wavelength within the *B*-line profile and dye laser 1 as a weaker scanning probe to detect changes of absorption produced by the pump. Detection is again via phonon sideband luminescence at 547 nm. Figure 5 shows data for sample UQWC21 at 1.5 K for two different positions within the *B*-line profile. The spectra were obtained by averaging the signal from  $\sim 128$  repeated frequency scans of the probe laser lasting  $\sim 1$  s each and then subtracting the same number of scans with the pump beam blocked. The change of absorption at the center of the hole is of the order a few percent in each case. Although the signal-to-noise ratio of the data did not allow a detailed

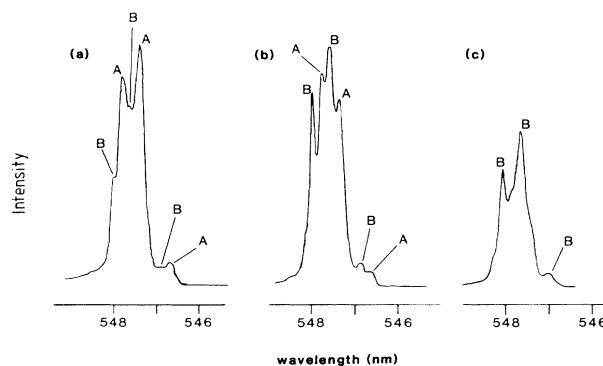


FIG. 4. Detail of phonon sideband luminescence of [Fig. 1(a)] for resonant excitation at three wavelengths within the *B*-state inhomogeneous profile; (a) 534.98 nm, (b) 535.11 nm, and (c) 535.16 nm. Sidebands of *A* and *B* zero-phonon lines are indicated.

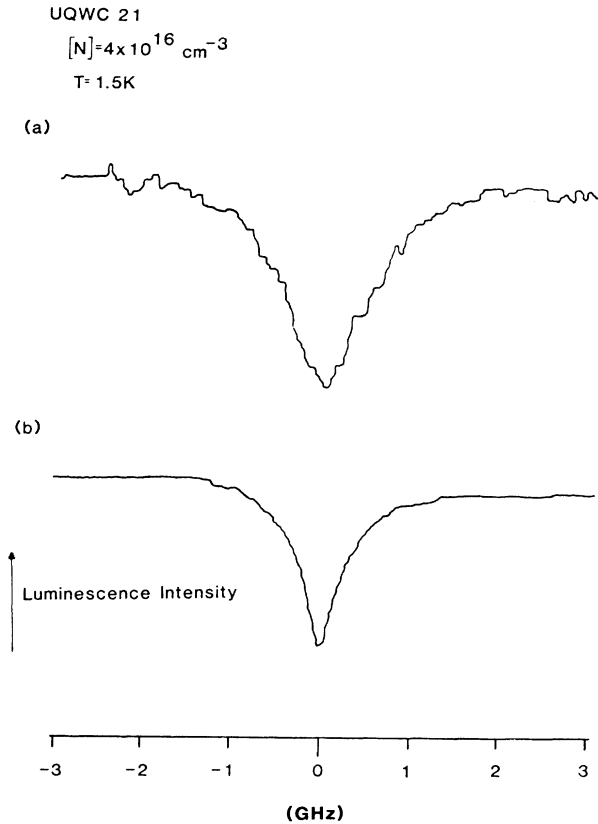


FIG. 5. Representative saturation holes measured in a sample with  $[N]=4 \times 10^{16} \text{ cm}^{-3}$  at 1.5 K at two positions within the *B*-state inhomogeneous envelope; (a) 535.07 nm and (b) 535.19 nm. The abscissa is the frequency of the probe laser relative to that of the pump. Laser power densities were pump  $\sim 4 \text{ W cm}^{-2}$  and probe  $\sim 1 \text{ W cm}^{-2}$ .

analysis of the shape of the holes, we did not observe large departures from Lorentzian behavior. We have quantified the data in terms of the measured hole widths at half height. These were independent of incident laser powers over the range 0.7 to  $16 \text{ W cm}^{-2}$  and were much greater than the laser linewidths.

In excitonic systems of this type in which the wave function extends over many unit cells and in which the binding center is a simple substitutional defect, we expect to observe only two-level saturation hole burning with hole lifetime limited by the upper-level decay. We established that the hole lifetime was much less than  $\sim 0.1 \text{ s}$  and may indeed be limited by the *B*-state decay ( $\sim 4 \mu\text{s}$ ).<sup>7</sup> Under these conditions the homogeneous optical linewidth  $\Gamma_{\text{hom}}$  is equal to half the hole width and the optical dephasing time is  $T_2 = (\pi\Gamma_{\text{hom}})^{-1}$ . Figure 6 shows the temperature dependence of hole width for UQWC21 for pump laser at 535.07 nm, close to the *B*-line center. Above 2 K there is a strong thermally activated temperature dependence, whereas below 2 K the hole width becomes approximately temperature independent at a value of about 800 MHz. Figure 7 shows the variation with pump wavelength of this temperature-independent width measured at 1.5 K for samples

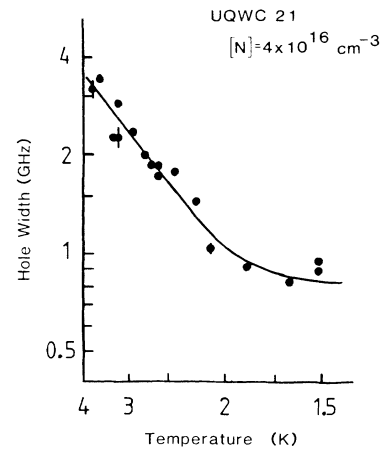


FIG. 6. Temperature variation of hole width in sample with  $[N]=4 \times 10^{16} \text{ cm}^{-3}$  at 535.07 nm, near the *B*-state line center. The solid curve is given by Eq. (1) with  $\Gamma_0=45 \text{ GHz}$ ,  $\Delta E=0.88 \text{ meV}$ , and  $\Gamma_1=0.75 \text{ GHz}$ .

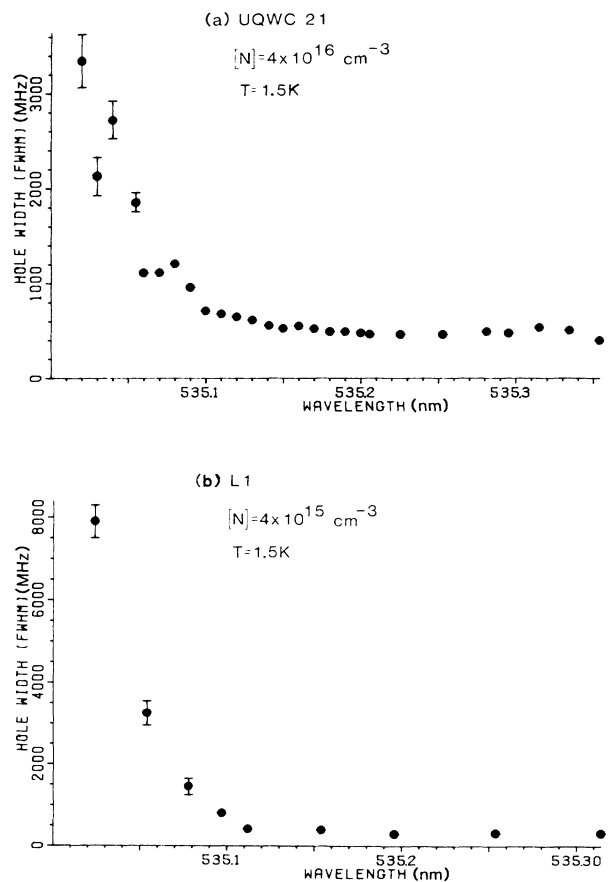


FIG. 7. Wavelength dependence of hole width at 1.5 K for samples with (a)  $4 \times 10^{16} \text{ N cm}^{-3}$  and (b)  $4 \times 10^{15} \text{ N cm}^{-3}$ . *B*-line center is at  $535.075 \pm 0.015 \text{ nm}$ .

UQWC21 and L1. Both samples show a rapid increase of hole width at energies just above line center of the  $B$  state and an approximately constant value in the low-energy tail of the line. In this region the widths for the more weakly doped sample L1 are approximately a factor of 2 less than those for UQWC21: The ratio of nitrogen concentrations is a factor of 10 (see Table I).

### III. DISCUSSION

#### A. Temperature dependence

The temperature dependence of hole widths observed above 2 K (see Fig. 6) is consistent with a thermally activated dephasing mechanism involving phonon-induced transitions from the  $B$  to the  $A$  state. The  $A$ - $B$  separation is  $\Delta E = 0.88$  meV. The solid curve, which gives a satisfactory description of the data in Fig. 6, has the form

$$\Gamma = \Gamma_0 e^{-\Delta E/kT} + \Gamma_1, \quad (1)$$

where  $\Gamma_0 = 45$  GHz and  $\Gamma_1 = 0.75$  GHz. The value of the prefactor,  $\Gamma_0$ , may be varied by  $\pm 5$  GHz without appreciably worsening the fit. We may compare this value of  $\Gamma_0$  with that derived from the echo experiments of Molenkamp and Wiersma<sup>4</sup> on the  $A$  state. At low temperatures they find that the dominant dephasing process for the  $A$  states is phonon-assisted  $A$  to  $B$  transitions which limit the  $A$ -state lifetime to  $25.5 \pm 0.5$  ps. Allowing for the relative degeneracies of  $A$  and  $B$  states, this gives a predicted value of  $\Gamma_0$  of  $7.5 \pm 0.15$  GHz, a factor of 6 less than our values. We shall return to discuss this difference in Sec. II D.

#### B. Temperature independent hole width

The temperature-independent part of the whole width measured at 1.5 K (Fig. 7), indicates dephasing times of order 800 ps or faster and shows a rapid increase at energies just above the  $B$ -line center. Several possible mechanisms for this dephasing may be envisaged. (i) Random inhomogeneities of the crystal could cause small unresolved splittings of the fivefold-degenerate  $B$  state leading to dephasing due to phonon-induced transitions among the components. Average strain splittings of order 0.4 meV would be required to explain the shift between absorption and emission (Fig. 3), a rather large value. Furthermore, hole-burning studies of the  $NN_1$  center,<sup>12</sup> for which the dominant dephasing mechanism is due to phonon-induced transitions among the crystal-field-split components of the  $B$  state, show hole widths of only 140 MHz. We therefore conclude that this dephasing mechanism is relatively unimportant in the present case, although it may become significant for the lowest nitrogen concentration (see below). (ii) We can rule out the possibility that the rapid increase of hole width near the line center is due to a mobility edge for the excitons, with extended delocalized states at higher energies and localized states below. This effect is found in other disordered systems, for example quasi-two-dimensional excitons in quantum wells<sup>2</sup> and GaAs:P.<sup>14</sup> It seems unlikely in the present case because of the low

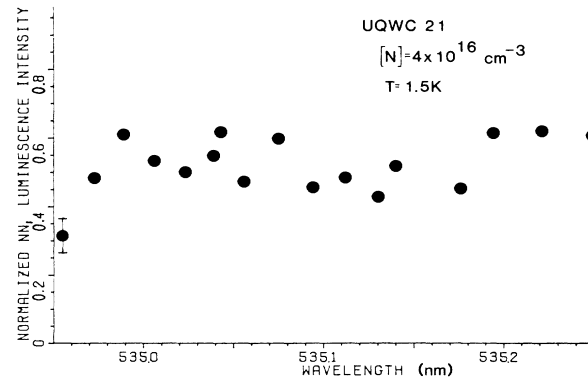


FIG. 8. Ratio of  $NN_1$  line emission to  $B$ -line absorption for excitation at different wavelengths within the  $B$  line, for  $[N] = 4 \times 10^{16} \text{ cm}^{-3}$ . Line center is at 535.075 nm.

nitrogen concentrations; the mean spacing of nitrogen impurities ( $> 300 \text{ \AA}$ ) is approximately an order of magnitude larger than the exciton radius. In addition, delocalization of the  $B$ -state exciton wave functions should result in enhanced trapping and emission at more tightly bound centers, principally  $NN_1$ , but this is not observed; in Fig. 8 we show the measured ratio of  $NN_1$  emission to  $B$ -line absorption in sample UQWC21 at 1.5 K as a function of excitation wavelength within the  $B$ -line profile. The data show some scatter but the ratio is effectively constant, indicating that there is no change in the nature of exciton states corresponding with the rapid variation of hole width. (iii) The observed hole width may be understood qualitatively, and to some extent quantitatively, in terms of phonon-assisted hopping or tunneling of excitons between neighboring nitrogen centers in the  $B$  state. At low temperatures, such migration predominantly involves loss of energy (i.e., phonon emission) so that the probability of hopping from a particular center is approximately proportional to the integrated density of states to lower energies. This quantity must fall rapidly with energy near to line center and can account for the rapid change in hole width observed. Such a mechanism is also consistent with the shift of emission relative to absorption noted in Fig. 3, and with the reduction of hole widths with nitrogen content between samples UQWC21 and L1.

We have made computer simulations of the dephasing rates based on this phonon-assisted hopping mechanism using the theories of Miller and Abrahams<sup>15</sup> and of Emin.<sup>16</sup> Assuming that there is no correlation between the energy of a particular site within the inhomogeneous profile and its location in the crystal, the hopping probability for an exciton from site  $i$  of energy  $E_i$  to site  $f$  of energy  $E_f$  a distance  $r$  away and, where the energy difference is taken up by one phonon, is

$$U_{ij} = C |E_f - E_i| \times \left\{ \frac{n+1}{n} \right\} \times r^2 \exp(-2r/a_0). \quad (2)$$

$C$  is a constant,  $n$  the Bose-Einstein factor for energy  $|E_f - E_i|$ , and  $a_0$  is the exciton radius. The factors

$n + 1$  and  $n$  refer to phonon emission and absorption, respectively. From the work of Emin<sup>16</sup> it can be shown that two-phonon and higher-order processes are not important in this case. The total hopping rate out of states with energy  $E_i$  may be calculated by integrating Eq. (2) over all energies ( $E_f$ ) and distances ( $r$ ), assuming a form for the density of final states  $E_f$ . We also assume that the centers are regularly distributed in space. Figure 9 shows the result of one such calculation. The calculated hole width is shown by the solid line, and the inhomogeneous line shape used in the calculation is shown by the dotted line. The purpose of the extra density of states to lower energy is to simulate the perturbed states which form the  $V$  band<sup>8</sup> [see Fig. 1(a)]. The calculation reproduces qualitatively the observed rapid change near line center. The temperature was set equal to 1.5 K in the calculation of Fig. 9. Similar calculations for higher temperatures show only a weak temperature dependence as expected from the form of Eq. (2).

Integration of Eq. (2) over  $r$  gives total hopping rates proportional to nitrogen concentration. As noted at the end of Sec. II, the ratio of hole widths for samples UQWC21 and L1 is approximately 2, whereas their nitrogen concentration ratio is  $\sim 10$  with experimental error of order  $\pm 50\%$  (see Table I). This discrepancy may be a result of the assumptions of the calculation, but may also indicate a contribution from a dephasing mechanism other than exciton migration, for example phonon-induced intra- $B$ -state transitions as described at the beginning of this section.

We have also made numerical estimates of the value of the constant  $C$ , given explicitly by Miller and Abrahams<sup>15</sup> and Emin,<sup>16</sup> using known physical constants for GaP. The result is a total hopping rate at line center, for nitrogen concentration of  $4 \times 10^{16} \text{ cm}^{-3}$ , approximately 70 times less than that determined experimentally for sample UQWC21. For such a calculation this represents acceptable agreement; small changes in the values of constants, particularly the bound exciton ra-

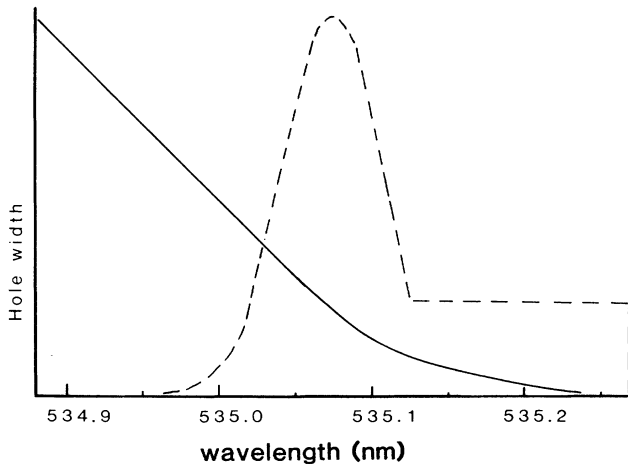


FIG. 9. Calculated variation of hole width due to exciton hopping with position within the  $B$  inhomogeneous line profile. For details see text.

dus which is not accurately known, would remove the discrepancy.

There are two other points, not covered by the calculations, which could be significant. First, the exciton-hopping probability to an  $NN_1$  pair will be enhanced compared to that to isolated nitrogen due to its greater binding energy through the factor  $|E_f - E_i|$  in Eq. (2). Thus the simple calculation will tend to underestimate the total hopping rate. Secondly, the calculated rate is an average over sites, there being a considerable variation from site to site. Experiments will clearly measure some form of weighted average which could be different. We expect that hole burning will give a value reasonably close to the unweighted average; however, the accumulated grating echo technique gives a very much lower value, as discussed in Sec. III D.

We conclude that the temperature-independent part of the hole width and also the observed shift of emission relative to absorption can be assigned to one-phonon-assisted hopping of excitons between different nitrogen binding centers within the inhomogeneous  $B$ -line profile.

### C. Comparison with hole burning in $NN_1$ centers

The importance of dephasing due to exciton hopping for single nitrogen centers at concentrations  $[N] = 4 \times 10^{15} \text{ cm}^{-3}$  (sample L1) may be contrasted with the case of  $NN_1$  pairs in concentrated material with  $[N] = 1.5 \times 10^{18} \text{ cm}^{-3}$  and  $[NN_1] \approx 5 \times 10^{14} \text{ cm}^{-3}$  (Ref. 12). In the latter case interpair hopping is not a significant dephasing mechanism and measured hole widths are ( $\sim 140 \text{ MHz}$ ) considerably less than for single nitrogen centers. Two reasons for the difference are, firstly the lower concentration of pairs than single ions, and secondly that the greater binding energy of the  $NN_1$  bound exciton will result in smaller radius and therefore less overlap with neighboring sites.

### D. Comparison with photon echo results for the $A$ state

Molenkamp and Wiersma<sup>4</sup> have made optical dephasing measurements in the  $A$  state using picosecond accumulated grating echo techniques. At low temperatures the dominant mechanism is decay from  $A$  to  $B$  accompanied by phonon emission; the measured rate was  $25.5 \pm 0.5 \text{ ps}$ , giving a value of  $\Gamma_0 = 7.5 \text{ GHz}$  for the reverse  $B$  to  $A$  process in Eq. (1) (see Sec. III A). Our measured value is  $\Gamma_0 = 45 \pm 5 \text{ GHz}$ . A second apparent discrepancy between our results and those of Molenkamp and Wiersma is the order of magnitude of the  $B$ -state dephasing time; the magnitude of their echo signals indicates a dephasing time of order of 100 ns for the  $B$  state, whereas our hole widths indicate times of order of 800 ps.

It is unlikely that these differences arise from sample differences since both Molenkamp and Wiersma and ourselves have used samples from a variety of sources and with nitrogen concentrations in the range  $10^{15} - 10^{17} \text{ cm}^{-3}$ , and have not found large sample-to-sample variations. We suggest that these apparent discrepancies can be understood as a consequence of the random statistical

nature of nitrogen distribution and differences in the two measurement techniques. As a result of the random distribution there will be a distribution of exciton-hopping rates resulting in different  $B$ -state dephasing times for different sites. Hole burning will tend to give an average value for dephasing time over this distribution. On the other hand, to observe an accumulated echo signal from the  $A$  state, a long dephasing time in the storage level (in this case the  $B$  state) is required. Thus the echo technique will tend to pick out from the distribution a subset of the centers which are truly isolated and have exceptionally low hopping probability. If this subset is assumed to dephase by radiative decay of the  $B$  state rather than by hopping it is possible to estimate that approximately 10% of the centers contribute to the echo signal in Molenkamp and Wiersma's experiment, the remainder having too short coherence time in the  $B$  state. It is also likely that such a select subset of centers may have a different  $A$ - $B$  phonon-assisted transition rate from the average, thereby accounting for the different values of  $\Gamma_0$  from the two experiments. The fact that the echo decays observed by Molenkamp and Wiersma are accurately exponential is consistent with the hypothesis that their experiment selects truly isolated centers.

#### IV. SUMMARY

We have used saturation spectral hole-burning techniques to study optical dephasing mechanisms for the dipole-forbidden  $B$  state of an exciton bound to single ni-

trogen impurity in GaP. Above 2.0 K the dephasing is thermally activated with activation energy (0.88 meV) corresponding to the splitting between the  $B$  and the  $A$  states. Below 1.5 K temperature-independent dephasing is observed which we assign to one-phonon assisted hopping of excitons between different nitrogen centers. Hopping occurs on a time scale of  $\sim 800$  ps although the average spacing of centers is  $\sim 300$  Å. There is a rapid increase of hopping rate for centers at and above line center associated with increased density of final states. The hopping rate falls with nitrogen concentration.

From comparison of our results with those of Molenkamp and Wiersma,<sup>4</sup> we conclude that there is a rather wide distribution of hopping times for different centers. The accumulated grating-echo technique detects signals from a small fraction ( $\sim 0.1$ ) of the centers, which are isolated and for which the dephasing time is close to the  $B$ -state radiative lifetime (4  $\mu$ s). In contrast, hole burning yields dephasing times of order 800 ps, which are determined by exciton migration. This presumably represents an average hopping time for excitons bound to the remaining, less-well-isolated centers.

#### ACKNOWLEDGMENTS

We thank M. D. Sturge and E. C. Lightowlers for providing samples used in these measurements and B. Movaghar for helpful discussions.

<sup>1</sup>W. H. Knox, R. L. Fork, M. C. Downer, D. A. B. Miller, D. S. Chemla, C. V. Shank, A. C. Gossard, and W. Weigmann, *Phys. Rev. Lett.* **54**, 1306 (1986).

<sup>2</sup>J. Hegarty, L. Goldner, and M. D. Sturge, *Phys. Rev. B* **30**, 7346 (1984).

<sup>3</sup>H.-J. Polland, L. Schultheis, J. Kuhl, E. O. Göbel, and C. W. Tu, *Phys. Rev. Lett.* **55**, 2610 (1985).

<sup>4</sup>L. W. Molenkamp and D. A. Wiersma, *Phys. Rev. B* **32**, 8108 (1985).

<sup>5</sup>R. M. Macfarlane, R. T. Harley, and R. M. Shelby, *Radiat. Eff.* **72**, 1 (1983).

<sup>6</sup>D. G. Thomas and J. J. Hopfield, *Phys. Rev.* **150**, 680 (1966).

<sup>7</sup>J. D. Cuthbert and D. G. Thomas, *Phys. Rev.* **154**, 763 (1967).

<sup>8</sup>D. Gershoni, E. Cohen, and A. Ron, *J. Lumin.* **34**, 83 (1985).

<sup>9</sup>P. J. Weisner, R. A. Street, and H. D. Wolf, *Phys. Rev. Lett.* **35**, 1366 (1975).

<sup>10</sup>*Proceedings of the International and Symposium on Rare Earth Spectroscopy, Polish Academy of Sciences, Technical University of Wrocław, University of Wrocław, Poland, 1984*, edited by B. Jezowska-Trzebiakowska, J. Lengendziewicz, and W. Strek (World Science, Singapore, 1985), pp. 563–568.

<sup>11</sup>P. J. Weisner, R. A. Street, and H. D. Wolf, *J. Lumin.* **12/13**, 265 (1976).

<sup>12</sup>R. T. Harley and R. M. Macfarlane, *J. Phys. C* **16**, L1121 (1983).

<sup>13</sup>E. C. Lightowlers, J. C. North, and O. G. Lorimor, *J. Appl. Phys.* **45**, 2191 (1974).

<sup>14</sup>D. Gershoni, E. Cohen, and A. Ron, *Phys. Rev. Lett.* **56**, 2211 (1986).

<sup>15</sup>A. Miller and E. Abrahams, *Phys. Rev.* **120**, 745 (1960).

<sup>16</sup>D. Emin, *Phys. Rev. Lett.* **32**, 303 (1974).